
Principled SVD-based Delta Compression via Quantization Error Minimization

Boya Xiong¹ Shuo Wang² Weifeng Ge³ Guanhua Chen⁴ Yun Chen¹

Abstract

Supervised Fine-Tuning (SFT) empowers Large Language Models (LLMs) with exceptional performance on specialized tasks, but it yields dense, high-dimensional delta parameters that pose severe storage and distribution challenges. Singular Value Decomposition (SVD)-based compression offers a compact representation for such delta parameters, but existing methods adopt heuristic quantization without clarifying underlying mechanisms, leading to poor generalizability. In this work, we propose PRINMIX, a rigorous SVD-based framework that models quantization as an optimization problem, grounding the design in mathematical mechanisms. We first theoretically derive quantization error and identify a key singular-value-dominated scaling mechanism, which mathematically proves the necessity of mix-precision quantization. We then model the quantization scheme as a 0/1 Integer Linear Programming (ILP) problem, which yields optimal bit-budget-constrained solutions without empirical assumptions. Furthermore, PRINMIX integrates a Reconstruction Target Correction (RTC) method to compensate for errors from the V-then-U sequential quantization process. Extensive experiments confirm PRINMIX performs well: for 7B LLMs, PRINMIX outperforms SOTA Delta-CoMe on challenging benchmarks by 22.3% on AIME2024 and 6.1% on GQA.

1. Introduction

Large language models (LLMs) have shown breakthrough performance on various knowledge-intensive (Grattafiori et al., 2024; Team, 2024; Jiang et al., 2023) and complex reasoning tasks (DeepSeek-AI, 2025; Grattafiori et al., 2024). Enhancing deployment efficiency is crucial for facilitating

LLM applications on edge devices and in cloud environments (Yao et al., 2024). In multi-tenant serving scenarios, multiple users fine-tune the same base model using their customized datasets (Wei et al., 2024; Yu et al., 2023), resulting in a variety of customized models that share a common foundation. These models, derived from the same base LLM (e.g., Qwen2.5 (Team, 2024) or LLaMA (Grattafiori et al., 2024)), need to be deployed concurrently to address simultaneous user requests. Conventional LLM compression approaches (Frantar et al., 2022; Lin et al., 2024) focus on quantizing and compressing the full model parameters. While effective at low compression ratios, these methods struggle to maintain model performance at high compression ratios, resulting in significant storage and computational overhead when deploying multiple customized LLMs.

In contrast to full model compression, delta-compression (Yao et al., 2024; Liu et al., 2024; Ping et al., 2024) decomposes a customized LLM into two components: the base model and the delta weights, which encapsulate the differences between the customized model and its corresponding base model. This approach emphasizes the compression of delta weights. Consequently, in multi-tenant environments, a single base model can be deployed alongside multiple sets of compressed delta parameters. Delta-compression achieves significantly higher compression rates than full model compression, thereby substantially reducing overall deployment costs. Researchers have explored effective approaches for delta-compression. Ryu et al. (2023) proposes a 1-bit quantization approach, termed BitDelta, to reduce the size of delta weights. Liu et al. (2024) leverages the low-rank characteristics of delta weights to improve storage efficiency through low-rank approximation. Delta-CoMe (Ping et al., 2024) introduces a mixed-precision delta-compression technique based on singular value decomposition (SVD), allocating higher-bit representations to singular vectors associated with larger singular values. Although these existing approaches demonstrate promising performance at high compression ratios, they lack rigorous mathematical foundations, which can lead to suboptimal performance, especially in challenging compression scenarios.

In this work, we propose PRINMIX, a high-performance principled mixed-precision delta-compression framework grounded in a solid theoretical foundation. PRINMIX implements delta-compression within the SVD space, formulating

¹Shanghai University of Finance and Economics ²Tsinghua University ³Fudan University ⁴Southern University of Science and Technology. Correspondence to: Guanhua Chen <chengh3@sustech.edu.cn>, Yun Chen <yunchen@sufe.edu.cn>.

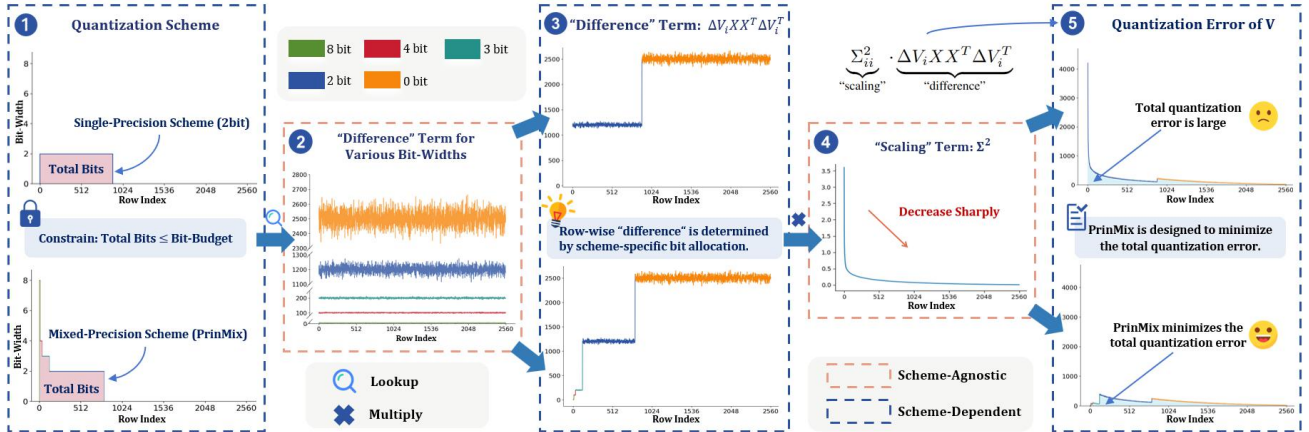


Figure 1. An overview of PRINMIX compared to single-precision quantization. Given the quantization scheme (①), we compute the “difference” term (③) by looking up the corresponding values in subfigure ②. The quantization error of the i -th row of \mathbf{V} comprise two components: a “scaling” term (④) and a “difference” term (③). PRINMIX identifies the optimal quantization scheme within the constraints of the bit budget (①) to effectively balance these two components, thereby minimizing the total quantization error of \mathbf{V} (⑤). Note that the “difference” term for various bit-widths (②) is pre-computed using a calibration dataset and remains fixed during the optimization process.

the quantization objective as the minimization of layer-wise quantization error. By pursuing this objective, PRINMIX establishes a mathematically sound mixed-precision compression strategy that accommodates flexible, user-defined compression ratios. This strategy derives **the mixed-precision scheme** through the solution of a 0/1 linear integer programming problem and ensures optimization consistency throughout the quantization process via a **reconstruction target correction method**. Unlike Ping et al. (2024), which empirically posits that singular vectors corresponding to larger singular values are more significant and, therefore, necessitate higher-bit representations, PRINMIX prioritizes the minimization of quantization error. It formulates all subsequent strategies based exclusively on this principle, eschewing reliance on singular values for assessing importance. This distinction is vital, as prior research has demonstrated that the significance attributed to singular values may not correlate with the performance of LLMs (Hsu et al., 2022; Wang et al., 2025).

We conduct extensive experiments on reasoning, math, code, and multimodal tasks across eight aligned LLMs to demonstrate the effectiveness of PRINMIX. The results show that PRINMIX achieves state-of-the-art performance among delta-compression methods, particularly in challenging scenarios where the norm of $\Delta\mathbf{W}$ is large. Notably, on the reasoning task AIME2024, PRINMIX surpasses the leading baseline, Delta-CoMe, by 22.3% on the 7B model and 26.9% on the 14B model. Furthermore, PRINMIX can achieve more than 6 \times GPU memory and disk storage savings, enabling the deployment of multiple models within constrained resource environments.

2. Related Work

Quantization Strategies for LLMs Quantization reduces the bit-precision of model parameters to lower GPU cost

and accelerate inference. Current strategies for LLM quantization can be broadly categorized into quantization-aware training (QAT) and post-training quantization (PTQ). QAT simulates quantization operations during training and uses backpropagation to correct quantization errors (Zhou et al., 2018; Esser et al., 2020; Liu et al., 2023b; Wang et al., 2023). In contrast, PTQ quantizes a pre-trained model without further training, typically calibrating the quantized weights with a modest calibration dataset (Dettmers et al., 2022; Frantar et al., 2022; Lin et al., 2024; Lee et al., 2024). Given the high computational cost associated with training or fine-tuning large language models, PTQ has become a particularly prevalent approach for LLM quantization. In our work, we leverage the GPTQ (Frantar et al., 2022) method within PTQ, focusing on mixed-precision quantization of the singular vectors of the delta parameters.

Delta-Compression Delta-compression (Isik et al., 2023; Ryu et al., 2023; Liu et al., 2024; Ping et al., 2024) aims to diminish the storage and inference costs associated with serving multiple models by compressing delta parameters, which are the differences between the parameters of a fine-tuned LLM and its corresponding base LLM. GPT-Zip (Isik et al., 2023) extends GPTQ to compress the delta parameters into 2-bit, and then sparsify 95% of the quantized delta weights to further reduce storage costs. DeltaZip (Yao et al., 2024) extends the idea of structured pruning and delta-compression to develop a multi-tenant serving system. However, both methods are still limited to compression ratios of 2-bit and higher. Liu et al. (2024) introduces BitDelta, which compresses delta weight into 1-bit, using a trainable high-precision scaling factor for each delta weight matrix. From this point onward, the compression of delta parameters has entered the 1-bit era. In addition to these low-bit methods, Ryu et al. (2023) identifies the low-rank property

Algorithm 1 Algorithm for Quantization in PRINMIX

Data: Delta parameter \mathbf{W} , List of candidate quantization bits Q , predefined averaged bit-width G_b , Calibration set X

Result: Quantized matrices $\hat{\mathbf{V}}$ and $\hat{\mathbf{U}}$

```

 $\mathbf{U}, \Sigma, \mathbf{V} \leftarrow \text{SVD}(\mathbf{W})$ 
for bit  $b$  in  $Q$  do
     $\mathbf{V}_b \leftarrow \text{SimQuant}(\mathbf{V}, b, X)$ 
     $\mathbb{E}_b^V \leftarrow \text{CalcLoss}(\mathbf{V}, \mathbf{V}_b, \Sigma)$ 
end
 $B \leftarrow \text{CalcStorage}(Q)$ 
 $S \leftarrow \text{SolveOpt}(B, G_b, \mathbb{E}^V)$ 
 $\hat{\mathbf{V}} \leftarrow \text{QuantParams}(\mathbf{V}, S, X)$ 
 $\tilde{\mathbf{U}} \leftarrow \text{RTC}(\mathbf{U}, \hat{\mathbf{V}}, \mathbf{V}, \Sigma, X)$ 
 $\hat{\mathbf{U}} \leftarrow \text{QuantParams}(\tilde{\mathbf{U}}, S, \hat{\mathbf{V}}, \Sigma, X)$ 
return  $\hat{\mathbf{V}}, \hat{\mathbf{U}}$ ; // Return results
    
```

of delta weights and achieves delta-compression through low-rank approximation. Recently, Delta-CoMe (Ping et al., 2024) leverages the benefits of both low-rank and low-bit compression methods, proposing a mixed-precision delta-compression method that uses varying bit-widths to represent different singular vectors of the delta weights. However, the rationale behind their mixed-precision quantization is predicated on a questionable hypothesis (Hsu et al., 2022; Wang et al., 2025): that singular vectors associated with larger singular values are inherently more important. This premise lacks a solid theoretical foundation, leading to a mixed-precision strategy that is primarily empirical and, consequently, suboptimal. In this work, we introduce PRINMIX, which provides a mathematical proof of the necessity for mixed-precision in SVD-based delta-compression methods, and derives a quantization approach that is firmly grounded in mathematical theory.

3. Method

In this section, we introduce PRINMIX, an adaptive mixed-precision delta-compression strategy for LLMs with mathematical support. In Section 3.1, we begin with the minimization of quantization error in the SVD space and derive the detailed \mathbf{V} -then- \mathbf{U} sequential quantization process. We provide a mathematical proof demonstrating the necessity of mixed-precision in this context. In Section 3.2, we present the detailed design of our mixed-precision scheme, which is formulated as a 0-1 Integer Linear Programming (ILP) problem. Algorithm 1 shows the details of PRINMIX.

3.1. Quantization Error Derivation

At a high level, PRINMIX follows the structure of the classical post-training quantization method GPTQ, by performing quantization to minimize the reconstruction error. Given a delta weight matrix \mathbf{W} and the corresponding input X , the quantization objective of the GPTQ is to find a quantized

matrix $\hat{\mathbf{W}}$ which minimizes the squared error:

$$\arg \min_{\hat{\mathbf{W}}} \left\| \mathbf{W}X - \hat{\mathbf{W}}X \right\|_F^2 = \sum_i \left\| W_i X - \hat{W}_i X \right\|_F^2 \approx \sum_i e_i \quad (1)$$

Following previous work (Hassibi et al., 1993; Nagel et al., 2020), the quantization error of the i^{th} row of \mathbf{W} can be approximated with a second-order Taylor expansion e_i :

$$e_i = \frac{1}{2} \Delta W_i \mathbf{H}_i \Delta W_i^T \quad (2)$$

Here $\Delta W_i = W_i - \hat{W}_i$ is the quantization difference of i^{th} row, while the Hessian matrix $\mathbf{H}_i = 2XX^T$ is independent and identical across different rows in \mathbf{W} . By reusing \mathbf{H} , GPTQ derives the optimal quantized weights $\hat{\mathbf{W}}$ row by row, allowing for parallel computation across multiple rows.

Instead of directly quantizing \mathbf{W} , PRINMIX performs quantization in the SVD space, by finding a quantized matrix $\hat{\mathbf{U}}$ and $\hat{\mathbf{V}}$ which minimizes the squared error:

$$\arg \min_{\hat{\mathbf{U}}, \hat{\mathbf{V}}} \left\| \mathbf{U}\Sigma\mathbf{V}X - \hat{\mathbf{U}}\Sigma\hat{\mathbf{V}}X \right\|_F^2 \quad (3)$$

where $\mathbf{W} = \mathbf{U}\Sigma\mathbf{V}$. Below, we introduce the detailed \mathbf{V} -then- \mathbf{U} sequential quantization process of PRINMIX, which first quantizes \mathbf{V} , and then moves to \mathbf{U} .

3.1.1. QUANTIZE \mathbf{V}

In this section, we present a theoretical analysis that motivates the need for mixed-precision quantization. Specifically, we find the quantized $\hat{\mathbf{V}}$ with the row-by-row approach by minimizing the squared error:

$$\arg \min_{\hat{\mathbf{V}}} \left\| \mathbf{U}\Sigma\mathbf{V}X - \mathbf{U}\Sigma\hat{\mathbf{V}}X \right\|_F^2 \approx \sum_i e_i^V \quad (4)$$

$$e_i^V = \frac{1}{2} \Delta V_i \mathbf{H}_i^V \Delta V_i^T$$

Here $\Delta V_i = V_i - \hat{V}_i$ is the quantization difference of the i^{th} row, and $\mathbf{H}_i^V = 2\Sigma_{ii}^2 \cdot XX^T$ is the Hessian matrix of the i^{th} row of \mathbf{V} (with derivation details in Appendix A.1). As Σ_{ii}^2 is a scalar, we can reformulate the Eq. (4) as follows:

$$e_i^V = \frac{1}{2} \Delta V_i \mathbf{H}_i^V \Delta V_i^T = \underbrace{\Sigma_{ii}^2}_{\text{"scaling"}} \cdot \underbrace{\Delta V_i X X^T \Delta V_i^T}_{\text{"difference"}} \quad (5)$$

From Eq. (5), it is evident that the error for i -th row of \mathbf{V} comprises two components: a “scaling” term Σ_{ii}^2 , which suggests that rows (singular vectors) with larger singular values has larger scaling factor, and a “difference” term

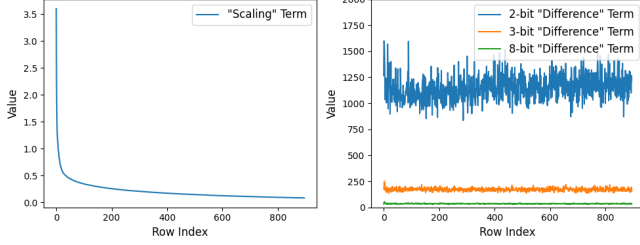


Figure 2. (Left) The value of “scaling” term (Eq. 5) at different row indices. (Right) The value of “difference” term (Eq. 5) with different quantization bit-width at different row indices. We compute all results using Q_Proj at the last layer of Qwen2.5-Math-7B-Instruct.

$\Delta V_i X X^T \Delta V_i^T$, derived from the quantization differences ΔV_i and limited sampling over a calibration set.

As illustrated in Figure 2, we present the results of the “scaling” and “difference” terms across different rows. The variation in the “difference” term remains relatively minor when the same bit-width is used to quantize different rows. In contrast, the “scaling” term decreases sharply as the row index i increases. Consequently, the quantization error e_i^V , which encompasses both terms, varies significantly across different rows under a uniform bit-width for quantization. To minimize the total error, it is ideal for the quantization error of each row to be small. Given that the “scaling” term is fixed for each row, we can only adjust the “difference” term by carefully allocating bit-widths. However, due to the constraints of the total bit budget, we cannot allocate high bit-widths to all rows simultaneously. Therefore, we propose a strategy of assigning varying bit-widths to different rows to reduce the overall quantization error. **Eq. (5) provides a theoretical foundation for the necessity of mixed-precision quantization in SVD-based delta-compression.** We discuss the detailed mixed-precision schedule in Section 3.2, which allocates varying bit-widths to different rows, specifically the different singular vectors of \mathbf{U} , by formulating a 0/1 integer linear programming problem.

3.1.2. QUANTIZE \mathbf{U}

In this section, we analyze why mixed-precision quantization is not crucial for \mathbf{U} . After quantizing \mathbf{V} to $\hat{\mathbf{V}}$, the quantization objective of \mathbf{U} is:

$$\begin{aligned} \arg \min_{\hat{\mathbf{U}}} \|\mathbf{U}\Sigma\hat{\mathbf{V}}X - \hat{\mathbf{U}}\Sigma\hat{\mathbf{V}}X\|_F^2 &\approx \sum_i e_i^U \\ e_i^U &= \frac{1}{2} \Delta U_i \mathbf{H}_i^U \Delta U_i^T = \Delta U_i \Sigma \hat{\mathbf{V}} X X^T \hat{\mathbf{V}}^T \Sigma^T \Delta U_i^T \end{aligned} \quad (6)$$

Here $\Delta U_i = U_i - \hat{U}_i$, and the Hessian matrix of the i^{th} row of \mathbf{U} is given by $\mathbf{H}_i^U = 2\Sigma\hat{\mathbf{V}}X X^T \hat{\mathbf{V}}^T \Sigma^T$ (with derivation details in Appendix A.2). Upon comparing Eq. (5) and Eq.

(6), we observe that e_i^U does not incorporate the scaling term present in Eq. (6). Consequently, when different rows are quantized using the same bit-width, there is no significant variation in error. This uniformity arises from the fact that the Hessian matrices for different rows of \mathbf{U} are identical. Thus, unlike \mathbf{V} , there is no necessity to employ mixed precision when quantizing different rows of \mathbf{U} .

Therefore, PRINMIX **determines the mixed-precision quantization schedule based on \mathbf{V}** , and then applies the same schedule to \mathbf{U} for simplicity. Specifically, PRINMIX quantizes \mathbf{U} using a column-wise mixed-precision schedule, where the i^{th} column of \mathbf{U} adopts the same bit-width as the i^{th} row of \mathbf{V} as they correspond to the same singular value. Notably, PRINMIX exhibits insensitivity to column-wise precision schedules, since GPTQ compensates for quantization-induced errors in the column direction by adjusting the unquantized weights during the quantization process. This compensation, however, does not occur between different rows, as different rows are independently quantized in GPTQ. This further underscores the importance of discussing row-wise mixed precision strategies aimed at minimizing the quantization error of \mathbf{V} . In Appendix C.1, we further demonstrate experimentally that applying the same mixed-precision quantization strategy to both \mathbf{V} and \mathbf{U} yields satisfactory performance.

Reconstruction Target Correction In Eq. (6), we quantize \mathbf{U} to reconstruct the target $\mathbf{U}\Sigma\hat{\mathbf{V}}X$, which deviates from the initial target $\mathbf{U}\Sigma\mathbf{V}X$. This deviation can negatively impact the performance of the quantized model. A straightforward approach to address this issue is to directly replace the reconstruction target with $\mathbf{U}\Sigma\mathbf{V}X$; however, this would inhibit the application of GPTQ for quantization, as it breaks the premise that GPTQ relies solely on second-order terms. Therefore, we propose a method termed “Reconstruction Target Correction” (RTC) to reduce the bias by transforming $\mathbf{U}\Sigma\hat{\mathbf{V}}X$ in Eq. (6) to $\tilde{\mathbf{U}}\Sigma\hat{\mathbf{V}}X$, where $\tilde{\mathbf{U}}$ is derived from the following equation:

$$\begin{aligned} \min_{\tilde{\mathbf{U}}} \|\mathbf{U}\Sigma\mathbf{V}X - \tilde{\mathbf{U}}\Sigma\hat{\mathbf{V}}X\|_F^2 \\ \Rightarrow \tilde{\mathbf{U}} = \mathbf{U}\Sigma\mathbf{V}X X^T \hat{\mathbf{V}}^T \Sigma^T (\Sigma\hat{\mathbf{V}}X X^T \hat{\mathbf{V}}^T \Sigma^T)^{-1} \end{aligned} \quad (7)$$

See Appendix A.3 for detailed derivations. In summary, prior to quantizing \mathbf{U} , we first update \mathbf{U} to $\tilde{\mathbf{U}}$ using Eq. (7). Subsequently, we perform quantization by minimizing $\|\tilde{\mathbf{U}}\Sigma\hat{\mathbf{V}}X - \hat{\mathbf{U}}\Sigma\hat{\mathbf{V}}X\|_F^2$. This approach aims to ensure that the reconstruction target closely approximates the original, without compromising the application of GPTQ for quantization.

3.2. Optimization Problem Modeling

In this section, we formulate the optimal mixed-precision bit allocation problem as a 0/1 integer linear programming

Table 1. Selected backbone and aligned models for the examined four tasks.

Task	7B Models		13-14B Models	
	Backbone	Aligned	Backbone	Aligned
Math	Qwen2.5-Math	Qwen2.5-Math-Instruct	LLaMA2	MetaMath
Reasoning	Qwen2.5-Math	DeepSeek-R1-Distill-Qwen	Qwen2.5	DeepSeek-R1-Distill-Qwen
Coder	Qwen2.5-Coder	Qwen2.5-Coder-Instruct	Qwen2.5-Coder	Qwen2.5-Coder-Instruct
Multi-Modal	Qwen2.5	Qwen2.5-VL-Instruct	LLaMA2	LLAVA-V1.5

model (see Eq. (8)). Given a user-specified compression target bit G_b , a candidate set of quantization bit-widths Q of size N_b , and an upper bound f_{\max} on the number of active bit-widths, the proposed model minimizes the quantization error by automatically selecting an subset of active bit-widths from Q , subject to the constraints imposed by G_b and f_{\max} .

As shown in Eq. (8), the objective is to minimize the total quantization error, expressed as $\sum_i \mathbb{E}_i^{\mathbf{V}} \mathcal{S}_i^T$. Here, $\mathbb{E}_i^{\mathbf{V}} \in \mathbb{R}^{1 \times N_b}$ denotes the quantization error associated with different bit-widths for the i^{th} row of \mathbf{V} , computed using predefined calibration data samples X_n in accordance with Eq. (4). $\mathcal{S}_i \in \mathbb{R}^{1 \times N_b}$ is a binary optimization variable indicating the selected bit-width for quantizing the i^{th} row of \mathbf{V} and the corresponding i^{th} column of $\tilde{\mathbf{U}}$. Note that our objective is limited to the quantization error of \mathbf{V} , with a detailed discussion provided in Sections 3.1.1 and 3.1.2.

$$\begin{aligned}
 & \min_{\mathcal{S}} \sum_i \mathbb{E}_i^{\mathbf{V}} \mathcal{S}_i^T \quad (\text{Total quantization error}) \\
 \text{s.t. } & \sum_i \mathcal{S}_i B \leq G_b (h_{\text{in}} \cdot h_{\text{out}}) \quad (\text{Bit budget constraint}) \\
 & \text{sum}(\mathcal{S}_i) = 1 \quad (\text{One-hot vector constraint}) \\
 & \mathcal{S}_i - f \leq 0 \quad (\text{Bit-width selection constraint}) \\
 & \text{sum}(f) \leq f_{\max} \quad (\text{Bit-width number constraint})
 \end{aligned} \tag{8}$$

The optimization problem has four constraints. (1) The “bit-budget constraint” ensures that the quantized model achieves a target compression bit that does not exceed the predefined threshold G_b . Here h_{in} and h_{out} represent the input and output dimension of \mathbf{W} . $B \in \mathbb{R}^{N_b \times 1}$ represents the storage required for quantizing a row of \mathbf{V} and a column of $\tilde{\mathbf{U}}$ at different bit-widths, which is computed as $B = (h_{\text{in}} + h_{\text{out}}) \cdot Q$. (2) The “one-hot vector constraint” requires that each row of \mathbf{V} and the corresponding column of $\tilde{\mathbf{U}}$ be quantized using exactly one bit-width. (3) The “bit-width selection constraint” guarantees that only permissible bit-widths are utilized for quantization. The variable $f \in \mathbb{R}^{1 \times N_b}$ denotes the set of admissible bit-widths, where $f_{0,k} = 1$ indicates that the k^{th} bit-width in Q is allowable. (4) The “bit-width number constraint” restricts the number of admissible bit-widths to a maximum of f_{\max} .

The 0/1 integer linear programming optimization prob-

lem is then solved with the CVXPY (Diamond & Boyd, 2016) library and the SCIP (Maher et al., 2016) solver. The Qwen2.5-Math-7B-Instruct model takes 29.4 minutes to solve, and this time can be further reduced by at least $4 \times$ by switching to a commercial solver (Ge et al., 2023) and reducing the solution space. We discuss this in detail in Appendix C.4.

By solving Eq. (8), we obtain an optimal mixed-precision scheme that minimizes the error while satisfying predefined bit budget constraints. This allows us to derive task-specific mixed-precision quantization strategies which balance the “scaling” and “difference” terms, leading to improved performance across various tasks.

4. Experiments

4.1. Experiment Setup

Evaluation Tasks We evaluate our methods on four distinct tasks: reasoning, math, code generation, and multi-modal. These tasks encompass a vast array of current directions based on fine-tuning with open-source LLMs. **Reasoning:** We use the Math500 and AIME2024 datasets as the test set. **Math:** We use the GSM8K (Cobbe et al., 2021) and Math500 (Lightman et al., 2023) datasets as the test set. **Code Generation:** We use HumanEval (Chen et al., 2021) and MBPP (Austin et al., 2021) as the test set. **Multi-Modal:** We utilize the GQA (Hudson & Manning, 2019) and the image part of ScienceQA (Lu et al., 2022) datasets. Please refer to Appendix B.1 for more details.

Models To ensure a comprehensive comparison, we evaluate both 7B and 13-14B models across the four tasks with various backbones, as shown in Table 1. During inference, we employ a greedy search strategy. Each model is compressed by a factor of 16 following (Ping et al., 2024) ($\alpha = 1/16$). In Appendix C.2, we report the performance of PRINMIX with different compression ratios.

Calibration Dataset Following Delta-CoMe (Ping et al., 2024), PRINMIX randomly samples 128 examples, each containing 2048 tokens, from the C4 training set as the calibration dataset. In Appendix C.3, we analyze the sensitivity of the calibration dataset by varying its domains and the number of examples. The results show that PRINMIX performs consistently well across different calibration dataset configurations.

Principled SVD-based Delta Compression via Quantization Error Minimization

Table 2. Comparison of PRINMIX and baselines on various tasks across 7B-sized models. We report the results in the format “mean(std)” with three runs for Delta-CoMe and PRINMIX.

Method	α	DeepSeek-R1-Distill-Qwen		Qwen2.5-Math-Instruct		Qwen2.5-Coder-Instruct		Qwen2.5-VL-Instruct		AVG
		Math500	AIME2024	Math500	GSM8K	Humaneval	Mbpp	GQA	SQA	
Backbone	1	70.6	16.7	70.6	84.8	72.0	80.7	-	-	-
Aligned	1	86.0	40.0	80.2	94.8	87.2	82.8	60.5	76.7	76.0
Low-Rank	1/16	72.2	13.3	59.6	70.3	84.1	86.2	0.0	0.0	48.2
BitDelta	1/16	1.4	0.0	71.2	84.0	83.5	83.9	0.0	0.3	40.5
Delta-CoMe	1/16	82.4(1.11)	30.0(3.30)	74.8(0.35)	94.5(0.00)	85.0(0.96)	82.7(0.17)	49.4(1.65)	76.5(0.26)	71.9
PRINMIX	1/16	82.7(0.83)	36.7(3.35)	77.7(1.03)	94.6(0.51)	85.6(0.35)	83.1(0.25)	52.4(2.30)	79.4(0.83)	74.0

Table 3. Comparison of PRINMIX and baselines on various tasks across 13-14B-sized models. We report the results in the format “mean(std)” with three runs for Delta-CoMe and PRINMIX.

Method	α	DeepSeek-R1-Distill-Qwen		MetaMath		Qwen2.5-Coder-Instruct		LLAVA-V1.5		AVG
		Math500	AIME2024	Math500	GSM8K	Humaneval	Mbpp	GQA	SQA	
Backbone	1	76.4	3.3	1.8	4.3	78.7	84.7	-	-	-
Aligned	1	87.4	40.0	22.6	71.0	90.2	85.4	63.3	72.8	66.6
Low-Rank	1/16	57.2	6.7	15.8	64.0	86.6	88.6	57.0	71.4	55.9
BitDelta	1/16	82.8	23.3	22.4	65.8	89.0	86.5	61.2	73.0	63.0
Delta-CoMe	1/16	76.5(3.38)	24.5(6.93)	22.9(0.12)	70.2(0.56)	90.6(0.75)	86.5(0.70)	62.8(0.09)	72.3(0.20)	63.3
PRINMIX	1/16	80.2(2.09)	31.1(3.81)	21.7(0.64)	71.2(0.26)	91.5(0.60)	86.9(0.12)	62.7(0.04)	72.1(0.18)	64.7

Table 4. Performance across different f_{\max} . We report the results in the format “mean(std)” with three runs.

Method	f_{\max}	DeepSeek-R1-Distill-Qwen-14B		AVG
		Math500	AIME2024	
Delta-CoMe	-	76.5(3.38)	24.5(6.93)	50.5
	2	80.7(1.75)	33.3(3.35)	57.0
	3	79.9(1.53)	30.0(8.83)	55.0
PRINMIX	4	80.2(2.09)	31.1(3.81)	55.7
	5	79.5(0.99)	33.3(6.65)	56.4
	6	79.5(2.21)	33.3(3.35)	56.4

Baselines We compare PRINMIX with three baselines: SVD-based low-rank compression (Ryu et al., 2023), BitDelta (Liu et al., 2024), and Delta-CoMe (Ping et al., 2024). All methods are evaluated using NVIDIA L20 GPUs.

4.2. Main Results

Tables 2 and 3 present the results of PRINMIX on both the 7B and 13-14B models across four tasks, in comparison to the baselines. Notably, PRINMIX demonstrates superior overall performance on both the 7B and 13-14B models, surpassing the best baseline, Delta-CoMe, by an average of 2.9% and 2.2%, respectively.

When analyzing the various tasks, we observe that PRINMIX exhibits more pronounced improvements in challenging scenarios characterized by a significant performance gap between the baseline methods and the aligned model. This is particularly evident in reasoning-intensive benchmarks, such as AIME2024, as well as in multimodal tasks utilizing 7B backbones. For instance, PRINMIX surpasses the previous state-of-the-art model, Delta-CoMe, by 22.3%

on the 7B model and by 26.9% on the 14B model. Further analysis reveals that these models display larger norms for $\Delta\mathbf{W}$. Specifically, the median norm of DeepSeek-R1-Distill-Qwen-7B and Qwen2.5-VL-Instruct is 6.5 and 10.3 times that of Qwen-Coder-Instruct-7B, with corresponding values of 26.13 and 41.45 compared to 4.02, respectively. In this context, baseline methods struggle to achieve optimal solutions due to their empirical nature. In contrast, PRINMIX directly optimizes quantization error from a mathematical perspective, enabling it to fully leverage its strengths in demanding tasks. However, on tasks where baselines already achieve near-lossless accuracy, such as MBPP and HumanEval on the 7B backbone, PRINMIX performs comparably to the best baseline. In these scenarios, the norm of $\Delta\mathbf{W}$ is relatively small and can be easily compressed, leading to a ceiling effect: $\Delta\mathbf{W}$ can be quantized almost losslessly by existing baselines, leaving little room for further improvement.

We also report the quantization time cost of PRINMIX. Please refer to Appendix C.4 for more details. The results show that PRINMIX requires only 1.1 hours for 7B models and 2.4 hours for 14B models on a single GPU. This time can be at least reduced by 2 \times by switching to a commercial solver and reducing the solution space, as discussed in C.4.

4.3. Ablation of f_{\max}

In PRINMIX, we set a hyperparameter termed f_{\max} to constrain the number of active bit-widths during quantization. This section examines the performance of PRINMIX under varying values of f_{\max} . As shown in Table 4, PRINMIX consistently achieves better performance than Delta-CoMe

Table 5. Ablation of RTC. We report the results in the format “mean(std)” with three runs.

	LLAVA-V1.5		DeepSeek-R1-Distill-Qwen-14B		AVG
	GQA	SQA	Math500	AIME2024	
Delta-CoMe	62.8(0.09)	72.3(0.20)	76.5(3.38)	24.5(6.93)	59.0
PRINMIX	62.7(0.04)	72.1(0.18)	80.2(2.09)	31.1(3.81)	61.5
PRINMIX (W/O RTC)	62.8(0.02)	72.2(0.05)	78.2(0.28)	27.5(3.81)	60.2

across all settings, indicating that PRINMIX is insensitive to the choice of f_{max} . In the main experiment, we set f_{max} to 4 to be consistent with Delta-CoMe.

4.4. Ablation of RTC

We conducted experiments to assess the necessity of RTC, as detailed in Table 5. Overall, RTC consistently enhances our method, yielding an average performance improvement of 2.2%. The results indicate that mitigating the deviation in the quantization loss of U enables PRINMIX to retain more information from ΔW . The importance of RTC is particularly pronounced in challenging tasks; for instance, it improves performance by 13.1% on the AIME2024 task. This improvement can be attributed to the more substantial quantization errors associated with quantizing V in these cases, thereby highlighting the critical need for reconstruction target correction.

5. Analyses

5.1. Delta-Compression vs. Delta-Tuning

Delta-compression decomposes the delta weights of a fully fine-tuned model into low-rank and low-bit representations, thereby reducing storage and inference costs. Delta-tuning methods, such as LoRA, are closely related to delta-compression but primarily aim to reduce the training costs of LLMs while achieving performance comparable to that of full fine-tuning. However, in various tasks—particularly more complex ones like code and math tasks—delta-tuning methods tend to underperform full fine-tuning (Biderman et al., 2024). This suggests that relying solely on delta-tuning may be insufficient.

In this section, we train the DeepSeek-LLM-7B-Base (DeepSeek-AI, 2024) on math and code tasks using both LoRA and full fine-tuning. We subsequently apply PRINMIX to the delta weights of the fully fine-tuned model and LoRA. Additional experimental details can be found in Appendix B.2. Table 6 presents a comparison of PRINMIX with LoRA. PRINMIX consistently outperforms LoRA across all tasks. When $\alpha = 1/16$, PRINMIX achieves an average score of 40.8, which is close to the aligned model’s score of 42.0, representing a 14.9% improvement over LoRA.

In addition to full fine-tuning model, PRINMIX can effectively compress the LoRA model as well. As illustrated

Table 6. Performance comparison between Delta-Compression and LoRA. Aligned is full fine-tuned model. For PRINMIX, we report the results in the format “mean(std)” with three runs.

Method	α	Code		Math		AVG
		Humaneval	Mbpp	Math500	GSM8K	
Backbone	1	24.4	46.0	3.8	14.7	22.2
Aligned	1	46.3	48.9	14.6	58.3	42.0
LoRA	1/16	34.1	47.7	9.4	50.9	35.5
PRINMIX	1/16	43.3(0.60)	50.2(0.82)	13.5(0.76)	56.1(0.82)	40.8
PRINMIX-LoRA	1/64	34.1(1.64)	47.7(0.85)	9.1(0.50)	49.7(0.30)	35.2
PRINMIX	1/64	39.4(1.56)	50.0(1.10)	11.1(0.95)	52.9(0.57)	38.4

in Table 6, PRINMIX-LoRA demonstrates a performance degradation of only 0.3 compared to the LoRA, while further compressing LoRA with a ratio of 4 ($\alpha = 1/64$). Notably, Baselines like BitDelta and Delta-CoMe cannot apply to LoRA. BitDelta directly quantizes ΔW to 1 bit without employing any low-rank approximation. Consequently, it cannot effectively utilize the low-rank properties inherent in LoRA. For Delta-CoMe, the empirically determined mixed-precision scheme is fixed and does not offer a clear method for allocating mixed precision at other compression ratios. In contrast, PRINMIX allows compression of ΔW to arbitrary ratios, making it more flexible and practically advantageous. Although PRINMIX-LoRA performs well on top of LoRA, it underperforms PRINMIX at the same compression ratio ($\alpha = 1/64$). This further highlights the significance of delta-compression in comparison to delta-tuning.

5.2. Inference Speed and Memory Cost

Following the setup of Liu et al. (2024), we evaluate the end-to-end decoding latency of Qwen2.5-7B variants using a single L20 GPU. As shown in Figure 3, we consider the setting where each deployed model receives one distinct request simultaneously—e.g., 12 deployed models correspond to a batch size of 12- with latency evaluation in three perspectives: (1) Memory Usage: This one measures peak GPU memory usage during concurrent inference, accounting for both model parameters and activation storage. (2) Prefill Time: This part focuses on the time the models take to process user-input prompts. Each request contains 512 input tokens, and we report the time (in ms) the model takes to handle them. (3) Generation Speed: This part evaluates how quickly the model generates output tokens (tokens/s) for each request. Since the prefill time already measures prompt processing, each request starts from the “[BOS]” token and generates 512 tokens sequentially.

As shown in Figure 3 (left), a single GPU can deploy only two aligned models simultaneously. In contrast, it can support up to 8 and 12 models concurrently for Delta-CoMe and PRINMIX, respectively. This enhancement is attributable to the fact that, as the number of models increases, both methods necessitate only the additional deployment of compressed delta weights, thereby significantly reducing mem-

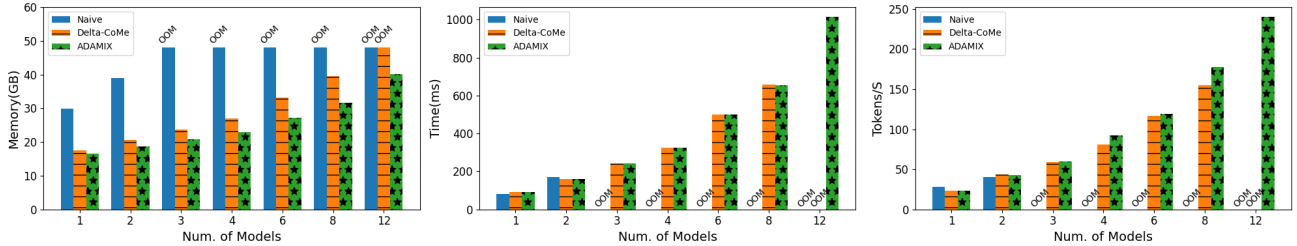


Figure 3. End-to-end decoding latency evaluation with varying numbers of deployed models using Qwen2.5-7B variants. (Left) Decoding memory usage. (Middle) Prefill time. (Right) Generation speed.

Table 7. Average quantization error ($\times 1e2$) on Qwen2.5-Math-7B-Instruct model with Eq. (1). “Low”, “Mid”, and “High” denote the first 9 layers, layers 9 to 17, and the last 10 layers, respectively. “All” and “Out” denote the average error across all activations and the average error of the top 1% of activations.

	Low		Mid		High	
	All	Out	All	Out	All	Out
Low-Rank	1.82	3.67	1.50	2.84	21.12	1890.34
BitDelta	2.18	2.81	0.61	1.08	21.51	3162.58
Delta-CoMe	0.76	1.79	0.75	1.33	7.54	470.82
PRINMIX	0.66	1.46	0.66	1.12	6.81	426.20

ory overhead. Notably, while Delta-CoMe exhausts GPU memory at 12 models, PRINMIX does not. Our further analysis indicates that PRINMIX typically employs fewer ranks, namely allocates a greater number of singular vectors with a bid-width of 0, thereby enhancing the GPU memory utilization efficiency.

For the end-to-end decoding latency illustrated in Figure 3 (middle, right), we find that Delta-CoMe and PRINMIX introduce overhead to Naive when the number of deployed model is small. However, Delta-CoMe and PRINMIX scale better and effectively translate the saved GPU memory into improved decoding latency. In contrast, the Naive approach quickly encounters out-of-memory issues. Furthermore, PRINMIX exhibits a superior generation speed compared to Delta-CoMe at scale, while the prefill times for both methods remain comparable. In Appendix C.6, we conduct more latency evaluation under varying arrival rates and request distributions following DeltaZip (Yao et al., 2024).

5.3. Analyzing Quantization Error

To better understand the difference between various delta-compression methods, we compute the quantization error on Qwen2.5-Math-7B-Instruct model as defined in Equation (1). Since outliers play a critical role in model compression (Dettmers et al., 2023; Lin et al., 2024), we also report the average error for the top 1% of activations with the largest absolute values in the aligned model, categorizing them as outliers. As different layers contribute differently to the final output (Wu et al., 2024), we categorize the first 9 layers, layers 9 to 17, and the last 10 layers as low, mid, and high

groups, respectively, and report the average error of each group. See Table 15 of Appendix C.8 for more details.

As demonstrated in Table 7, PRINMIX consistently exhibits lower overall quantization error compared to all baseline methods, attributable to its inherent objective of minimizing the quantization error. In the mid layers, PRINMIX shows a slightly higher error than the BitDelta, with values of 0.66 versus 0.61 for all activations and 1.12 versus 1.08 for outlier activations, respectively. However, it is important to note that since BitDelta is an empirical method, it cannot guarantee low quantization error across all layers. For example, in the high layers, BitDelta exhibits significantly higher error rates compared to PRINMIX, with values of 21.51 versus 6.81 for all activations and 3162.58 versus 426.20 for outlier activations, respectively. These experiments further illustrate that PRINMIX effectively reduces quantization error, thereby preserving the information contained in the delta weights as much as possible. In Appendix C.7, we visualize the bit allocation results of PRINMIX across different weight types and layers using the Qwen2.5-Math-7B-Instruct model.

6. Conclusion

In this study, we present PRINMIX, an adaptive mixed-precision delta-compression framework aimed at minimizing quantization error in the SVD space without introducing additional assumptions. PRINMIX offers a theoretical proof of the necessity for mixed-precision delta-compression and provides a practical quantization solution that involves solving a 0/1 linear integer programming problem and employing a reconstruction target correction method. PRINMIX outperforms all baseline delta-compression methods across four distinct downstream tasks, including reasoning, math, code, and multi-modal, utilizing eight widely adopted aligned LLMs with backbone pre-trained models, including Qwen2.5, Qwen2.5-Math, Qwen2.5-Coder, and LLaMA2. Moreover, PRINMIX significantly reduces deployment costs by minimizing memory overhead and accelerating inference. We believe that PRINMIX provides considerable theoretical and practical value, particularly in scenarios involving multi-tenant deployments.

Impact Statement

PRINMIX significantly reduces hardware requirements and computational costs for serving multiple finetuned models, thereby enabling smaller entities to deploy advanced large language models more feasibly. Additionally, it lowers power consumption and reduces the carbon emissions associated with LLM deployment. Despite PRINMIX’s demonstrated improvements over baseline methods in reducing the performance gap between compressed and aligned models, it is important to note that PRINMIX remains a lossy compression method for certain tasks. We believe this is an important consequence and encourage future research to further minimize this performance gap, particularly in tasks where performance degradation is substantial.

References

- Austin, J., Odena, A., Nye, M., Bosma, M., Michalewski, H., Dohan, D., Jiang, E., Cai, C., Terry, M., Le, Q., and Sutton, C. Program synthesis with large language models, 2021. URL <https://arxiv.org/abs/2108.07732>.
- Biderman, D., Portes, J., Ortiz, J. J. G., Paul, M., Greengard, P., Jennings, C., King, D., Havens, S., Chiley, V., Frankle, J., Blakeney, C., and Cunningham, J. P. Lora learns less and forgets less, 2024. URL <https://arxiv.org/abs/2405.09673>.
- Chen, M., Tworek, J., Jun, H., Yuan, Q., de Oliveira Pinto, H. P., Kaplan, J., Edwards, H., Burda, Y., Joseph, N., Brockman, G., Ray, A., Puri, R., Krueger, G., Petrov, M., Khlaaf, H., Sastry, G., Mishkin, P., Chan, B., Gray, S., Ryder, N., Pavlov, M., Power, A., Kaiser, L., Bavarian, M., Winter, C., Tillet, P., Such, F. P., Cummings, D., Plappert, M., Chantzis, F., Barnes, E., Herbert-Voss, A., Guss, W. H., Nichol, A., Paino, A., Tezak, N., Tang, J., Babuschkin, I., Balaji, S., Jain, S., Saunders, W., Hesse, C., Carr, A. N., Leike, J., Achiam, J., Misra, V., Morikawa, E., Radford, A., Knight, M., Brundage, M., Murati, M., Mayer, K., Welinder, P., McGrew, B., Amodei, D., McCandlish, S., Sutskever, I., and Zaremba, W. Evaluating large language models trained on code, 2021. URL <https://arxiv.org/abs/2107.03374>.
- Cobbe, K., Kosaraju, V., Bavarian, M., Chen, M., Jun, H., Kaiser, L., Plappert, M., Tworek, J., Hilton, J., Nakano, R., Hesse, C., and Schulman, J. Training verifiers to solve math word problems. *arXiv preprint arXiv:2110.14168*, 2021.
- DeepSeek-AI. Deepseek llm: Scaling open-source language models with longtermism. *arXiv preprint arXiv:2401.02954*, 2024. URL <https://github.com/deepseek-ai/DeepSeek-LLM>.
- DeepSeek-AI. Deepseek-r1: Incentivizing reasoning capability in llms via reinforcement learning, 2025. URL <https://arxiv.org/abs/2501.12948>.
- Dettmers, T., Lewis, M., Belkada, Y., and Zettlemoyer, L. Gpt3. int8 (): 8-bit matrix multiplication for transformers at scale. *Advances in Neural Information Processing Systems*, 35:30318–30332, 2022.
- Dettmers, T., Svirschevski, R., Egiazarian, V., Kuznedev, D., Frantar, E., Ashkboos, S., Borzunov, A., Hoefler, T., and Alistarh, D. Spqr: A sparse-quantized representation for near-lossless llm weight compression, 2023. URL <https://arxiv.org/abs/2306.03078>.
- Diamond, S. and Boyd, S. CVXPY: A Python-embedded modeling language for convex optimization. *Journal of Machine Learning Research*, 17(83):1–5, 2016.
- Esser, S. K., McKinstry, J. L., Bablani, D., Appuswamy, R., and Modha, D. S. Learned step size quantization, 2020. URL <https://arxiv.org/abs/1902.08153>.
- Frantar, E., Ashkboos, S., Hoefler, T., and Alistarh, D. Gptq: Accurate post-training quantization for generative pretrained transformers. *arXiv preprint arXiv:2210.17323*, 2022.
- Ge, D., Huangfu, Q., Wang, Z., Wu, J., and Ye, Y. Cardinal Optimizer (COPT) user guide. <https://guide.coap.online/copt/en-doc>, 2023.
- Grattafiori, A., Dubey, A., Jauhri, A., Pandey, A., and et al. The llama 3 herd of models, 2024. URL <https://arxiv.org/abs/2407.21783>.
- Hassibi, B., Stork, D., and Wolff, G. Optimal brain surgeon and general network pruning. In *IEEE International Conference on Neural Networks*, pp. 293–299 vol.1, 1993. doi: 10.1109/ICNN.1993.298572.
- Hsu, Y.-C., Hua, T., Chang, S., Lou, Q., Shen, Y., and Jin, H. Language model compression with weighted low-rank factorization, 2022. URL <https://arxiv.org/abs/2207.00112>.
- Hudson, D. A. and Manning, C. D. Gqa: A new dataset for real-world visual reasoning and compositional question answering, 2019. URL <https://arxiv.org/abs/1902.09506>.
- Isik, B., Kumbong, H., Ning, W., Yao, X., Koyejo, S., and Zhang, C. GPT-zip: Deep compression of finetuned large language models. In *Workshop on Efficient Systems for Foundation Models @ ICML2023*, 2023. URL <https://openreview.net/forum?id=h00c2tG2xL>.

- Jiang, A. Q., Sablayrolles, A., Mensch, A., Bamford, C., Chaplot, D. S., de las Casas, D., Bressand, F., Lengyel, G., Lample, G., Saulnier, L., Lavaud, L. R., Lachaux, M.-A., Stock, P., Scao, T. L., Lavril, T., Wang, T., Lacroix, T., and Sayed, W. E. Mistral 7b, 2023. URL <https://arxiv.org/abs/2310.06825>.
- Lee, C., Jin, J., Kim, T., Kim, H., and Park, E. Owq: Outlier-aware weight quantization for efficient fine-tuning and inference of large language models, 2024. URL <https://arxiv.org/abs/2306.02272>.
- Lightman, H., Kosaraju, V., Burda, Y., Edwards, H., Baker, B., Lee, T., Leike, J., Schulman, J., Sutskever, I., and Cobbe, K. Let’s verify step by step. *arXiv preprint arXiv:2305.20050*, 2023.
- Lin, J., Tang, J., Tang, H., Yang, S., Chen, W.-M., Wang, W.-C., Xiao, G., Dang, X., Gan, C., and Han, S. Awq: Activation-aware weight quantization for on-device llm compression and acceleration. *Proceedings of Machine Learning and Systems*, 6:87–100, 2024.
- Liu, J., Xia, C. S., Wang, Y., and Zhang, L. Is your code generated by chatGPT really correct? rigorous evaluation of large language models for code generation. In *Thirty-seventh Conference on Neural Information Processing Systems*, 2023a. URL <https://openreview.net/forum?id=1qvx610Cu7>.
- Liu, J., Xiao, G., Li, K., Lee, J. D., Han, S., Dao, T., and Cai, T. Bitdelta: Your fine-tune may only be worth one bit, 2024. URL <https://arxiv.org/abs/2402.10193>.
- Liu, Z., Oguz, B., Zhao, C., Chang, E., Stock, P., Mehdad, Y., Shi, Y., Krishnamoorthi, R., and Chandra, V. Llm-qat: Data-free quantization aware training for large language models, 2023b. URL <https://arxiv.org/abs/2305.17888>.
- Lu, P., Mishra, S., Xia, T., Qiu, L., Chang, K.-W., Zhu, S.-C., Tafjord, O., Clark, P., and Kalyan, A. Learn to explain: Multimodal reasoning via thought chains for science question answering. In *The 36th Conference on Neural Information Processing Systems (NeurIPS)*, 2022.
- Luo, H., Sun, Q., Xu, C., Zhao, P., Lou, J., Tao, C., Geng, X., Lin, Q., Chen, S., Tang, Y., and Zhang, D. Wizardmath: Empowering mathematical reasoning for large language models via reinforced evol-instruct, 2025. URL <https://arxiv.org/abs/2308.09583>.
- Maher, S., Miltenberger, M., Pedroso, J. P., Rehfeldt, D., Schwarz, R., and Serrano, F. PySCIPopt: Mathematical programming in python with the SCIP optimization suite. In *Mathematical Software – ICMS 2016*, pp. 301–307. Springer International Publishing, 2016. doi: 10.1007/978-3-319-42432-3_37.
- Nagel, M., Amjad, R. A., Van Baalen, M., Louizos, C., and Blankevoort, T. Up or down? adaptive rounding for post-training quantization. In *International Conference on Machine Learning*, pp. 7197–7206. PMLR, 2020.
- Naman Jain, King Han, A. G. and et al. Livecodebench: Holistic and contamination free evaluation of large language models for code. *arXiv preprint*, 2024.
- Ping, B., Wang, S., Wang, H., Han, X., Xu, Y., Yan, Y., Chen, Y., Chang, B., Liu, Z., and Sun, M. Delta-come: Training-free delta-compression with mixed-precision for large language models, 2024. URL <https://arxiv.org/abs/2406.08903>.
- Ryu, S., Seo, S., and Yoo, J. Efficient storage of fine-tuned models via low-rank approximation of weight residuals, 2023. URL <https://arxiv.org/abs/2305.18425>.
- Team, Q. Qwen2.5: A party of foundation models, September 2024. URL <https://qwenlm.github.io/blog/qwen2.5/>.
- Tillet, P., Kung, H.-T., and Cox, D. Triton: an intermediate language and compiler for tiled neural network computations. In *Proceedings of the 3rd ACM SIGPLAN International Workshop on Machine Learning and Programming Languages*, pp. 10–19, 2019.
- Wang, H., Ma, S., Dong, L., Huang, S., Wang, H., Ma, L., Yang, F., Wang, R., Wu, Y., and Wei, F. Bitnet: Scaling 1-bit transformers for large language models, 2023. URL <https://arxiv.org/abs/2310.11453>.
- Wang, X., Zheng, Y., Wan, Z., and Zhang, M. Svd-llm: Truncation-aware singular value decomposition for large language model compression, 2025. URL <https://arxiv.org/abs/2403.07378>.
- Wei, Y., Wang, Z., Liu, J., Ding, Y., and Zhang, L. Magicoder: Empowering code generation with oss-instruct, 2024. URL <https://arxiv.org/abs/2312.02120>.
- Wu, X., Huang, S., and Wei, F. Mixture of lora experts, 2024. URL <https://arxiv.org/abs/2404.13628>.
- Yao, X., Hu, Q., and Klimovic, A. Deltazip: Efficient serving of multiple full-model-tuned llms, 2024. URL <https://arxiv.org/abs/2312.05215>.
- Yu, L., Jiang, W., Shi, H., Yu, J., Liu, Z., Zhang, Y., Kwok, J. T., Li, Z., Weller, A., and Liu, W. Metamath: Bootstrap your own mathematical questions for large language models. *arXiv preprint arXiv:2309.12284*, 2023.

Zhang, K., Li, B., Zhang, P., Pu, F., Cahyono, J. A., Hu, K., Liu, S., Zhang, Y., Yang, J., Li, C., and Liu, Z. Lmms-eval: Reality check on the evaluation of large multimodal models, 2024. URL <https://arxiv.org/abs/2407.12772>.

Zhou, S., Wu, Y., Ni, Z., Zhou, X., Wen, H., and Zou, Y. Dorefa-net: Training low bitwidth convolutional neural networks with low bitwidth gradients, 2018. URL <https://arxiv.org/abs/1606.06160>.

A. Formula Derivation

A.1. V Hessian Matrix

$$\begin{aligned}
 & d_{\hat{V}}^2 \left\| \mathbf{U}\Sigma\mathbf{V}X - \mathbf{U}\Sigma\hat{\mathbf{V}}X \right\|_F^2 \\
 &= 2\text{tr}(\mathbf{U}\Sigma d\hat{\mathbf{V}}XX^T d\hat{\mathbf{V}}^T \Sigma^T \mathbf{U}^T) \\
 &= 2\text{tr}(\Sigma^T \mathbf{U}^T \mathbf{U}\Sigma d\hat{\mathbf{V}}XX^T d\hat{\mathbf{V}}^T) \\
 &= 2(d \text{vec}(\hat{\mathbf{V}}^T))^T (\Sigma^T \Sigma \otimes XX^T) (d \text{vec}(\hat{\mathbf{V}}^T)) \\
 &= 2(d \text{vec} \hat{\mathbf{V}})^T (\Sigma^T \Sigma \otimes XX^T) (d \text{vec}(\hat{\mathbf{V}})) \\
 &\Rightarrow \mathbf{H}^V = 2\Sigma^T \Sigma \otimes XX^T \\
 &\Rightarrow \mathbf{H}_i^V = 2\Sigma_{ii}^2 \cdot XX^T
 \end{aligned} \tag{9}$$

Here \otimes denotes the Kronecker product.

A.2. U Hessian Matrix

$$\begin{aligned}
 & d_{\hat{U}}^2 \left\| \mathbf{U}\Sigma\hat{\mathbf{V}}X - \hat{\mathbf{U}}\Sigma\hat{\mathbf{V}}X \right\|_F^2 \\
 &= d\hat{\mathbf{U}}\Sigma\hat{\mathbf{V}}XX^T \hat{\mathbf{V}}^T \Sigma^T d\hat{\mathbf{U}}^T \\
 &= X^T \hat{\mathbf{V}}^T \Sigma^T d\hat{\mathbf{U}}^T d\hat{\mathbf{U}}\Sigma\hat{\mathbf{V}}X \\
 &= (d \text{vec} \hat{U})^T \mathbf{K}_{\text{rhout}} (\mathbf{I} \otimes \Sigma \hat{\mathbf{V}}XX^T \hat{\mathbf{V}}^T \Sigma^T) \mathbf{K}_{\text{houtr}} (d \text{vec} \hat{U}) \\
 &= 2(d \text{vec} \hat{U})^T (\mathbf{I} \otimes \Sigma \hat{\mathbf{V}}XX^T \hat{\mathbf{V}}^T \Sigma^T) (d \text{vec} \hat{U}) \\
 &\Rightarrow \mathbf{H}_i^U = \mathbf{H}^U = 2\Sigma \hat{\mathbf{V}}XX^T \hat{\mathbf{V}}^T \Sigma^T
 \end{aligned} \tag{10}$$

Here $\mathbf{K}_{\text{houtr}}$ is the commutation matrix, and $\mathbf{K}_{\text{houtr}}^{-1} = \mathbf{K}_{\text{rhout}}$.

A.3. Detailed Derivation Process for new U

$$\begin{aligned}
 & d_{\tilde{U}} \left\| \mathbf{U}\Sigma\mathbf{V}X - \tilde{\mathbf{U}}\Sigma\hat{\mathbf{V}}X \right\|_F^2 \\
 &= 2\text{tr}(d\tilde{\mathbf{U}}\Sigma\hat{\mathbf{V}}X (\tilde{\mathbf{U}}\Sigma\hat{\mathbf{V}}X - \mathbf{U}\Sigma\mathbf{V}X)^T) \\
 &= 2\text{tr}(\Sigma \hat{\mathbf{V}}X (\tilde{\mathbf{U}}\Sigma\hat{\mathbf{V}}X - \mathbf{U}\Sigma\mathbf{V}X)^T d\tilde{\mathbf{U}}) \\
 &\Rightarrow \frac{\partial \mathbb{L}}{\partial \tilde{\mathbf{U}}} = (\tilde{\mathbf{U}}\Sigma\hat{\mathbf{V}}X - \mathbf{U}\Sigma\mathbf{V}X)X^T \hat{\mathbf{V}}^T \Sigma^T
 \end{aligned} \tag{11}$$

By setting the gradient of the loss to zero, PRINMIX gets the corrected $\tilde{\mathbf{U}}$ as follow:

$$\begin{aligned}
 & \frac{\partial \mathbb{L}}{\partial \tilde{\mathbf{U}}} = (\tilde{\mathbf{U}}\Sigma\hat{\mathbf{V}}X - \mathbf{U}\Sigma\mathbf{V}X)X^T \hat{\mathbf{V}}^T \Sigma^T = 0 \\
 & \Rightarrow \tilde{\mathbf{U}} = \mathbf{U}\Sigma\mathbf{V}XX^T \hat{\mathbf{V}}^T \Sigma^T (\Sigma \hat{\mathbf{V}}XX^T \hat{\mathbf{V}}^T \Sigma^T)^{-1}
 \end{aligned} \tag{12}$$

B. Experiments Setup

B.1. Main Experiments

We evaluate our methods across models in Table 1 on four distinct tasks: math, reasoning, code generation, and multi-modal. These tasks encompass a vast array of current directions based on fine-tuning with open-source LLMs.

- **Math.** We use the GSM8K (Cobbe et al., 2021) and Math500 (Lightman et al., 2023) datasets as the test set. We follow the prompt format of WizardMath (Luo et al., 2025) and set the maximum generation length to 1024. The evaluation metric is accuracy, determined by comparing the model-generated solution to the ground truth.

- **Reasoning.** We use the Math500 and AIME2024 datasets as the test set. For the reasoning prompt of AIME2024, we follow with (Naman Jain & et al., 2024). The maximum length of both tasks is set to 8192. The evaluation metric is accuracy, determined by comparing the model-generated solution to the ground truth.
- **Code Generation.** We use two widely used datasets as the test set: HumanEval (Chen et al., 2021) and MBPP (Austin et al., 2021). We follow the Magicoder (Wei et al., 2024) evaluation framework for HumanEval and adopt EvalPlus (Liu et al., 2023a) for MBPP. The evaluation metric is the pass rate (pass@1), which measures whether the code generated in a single attempt successfully passes the test cases.
- **Multi-Modal.** We utilize the GQA (Hudson & Manning, 2019) and the image part of ScienceQA (Lu et al., 2022) datasets, both commonly used for evaluating VLM performance, as our test set. We adopt Imms-eval (Zhang et al., 2024) to evaluate both tasks. The evaluation metric is accuracy, which measures whether the model selects the correct option.

B.2. Delta-Compression vs. Delta-Tuning

Specifically, we set the LoRA rank to 128 and the scale factor to 256, training LoRA for all model parameters for 3 epochs using a cosine schedule with a peak learning rate of 4e-5 and a warm-up ratio of 0.1, using model deepseek-llm-7b-base (DeepSeek-AI, 2024). We randomly sample 50k training examples from MetaMathQA (Yu et al., 2023) and Magicoder-Evol-Instruct (Wei et al., 2024) for the math and code tasks, respectively. To ensure a fair comparison, we fine-tune all model parameters using the same datasets as those used for LoRA training. We then apply PRINMIX to both math and code finetuned LLMs.

C. More Experiments

C.1. Analyzing the Different Quantization Schemes in U

In this section, we investigate the effect of applying different quantization schemes to U in order to assess the necessity of mixed precision. Our evaluation is conducted on Qwen2.5-Math-7B-Instruct. The results show that there is no significant difference between PRINMIX and other quantization methods for U . As shown in Table 8, “x-bit” denotes quantization of U with x-bit precision. The “PRINMIX-row” setting applies the optimization model to determine the scheme and performs quantization in a row-wise manner, whereas “PRINMIX” adopts the same quantization scheme as V and conducts quantization column by column. The performance differences across schemes are minimal, with the largest gap in average scores being only 0.95%, observed between the “PRINMIX-row” setting and the 2-bit quantization. These results suggest that the choice of quantization strategy for U has only a limited impact on overall performance.

Table 8. We evaluate the performance of various quantization schemes applied to U on Qwen2.5-Math-7B-Instruct. Here, “x-bit” denotes quantization of U at x-bit precision. The “PRINMIX-row” setting refers to applying the optimization model to determine the scheme and performing quantization in a row-wise manner, whereas “PRINMIX” indicates employing the same quantization scheme used for V , with quantization carried out column by column.

	α	Math500	GSM8K	AVG
U(2bit),V(PRINMIX)	1/16	76.8	93.6	85.2
U(3bit),V(PRINMIX)	1/16	75.6	93.4	84.5
U(PRINMIX-row),V(PRINMIX)	1/16	75.2	93.6	84.4
PRINMIX	1/16	75.2	93.9	84.6

C.2. Ablation of Compression Ratio

To show that PRINMIX can apply to arbitrary compression ratios, we evaluate Qwen2.5-Math-7B-Instruct at four compression ratios, as shown in Table 9. The performance of PRINMIX decreases as the compression ratio increases. This is expected, as a higher compression ratio indicates a reduced capacity of the quantized model to preserve information from the original model. Notably, baselines like BitDelta and Delta-CoMe cannot apply to other compression ratios except $\alpha = 1/16$. BitDelta quantizes ΔW to a fixed 1 bit, resulting in a constant compression ratio. For Delta-CoMe, the em-

Table 9. Performance of PRINMIX under different compression ratios $1/\alpha$.

Compression Ratio	DeepSeek-R1-Distill-Qwen-7B		Qwen2.5-Math-7B-Instruct			
	α	Math500	AIME2024	Math500	GSM8K	AVG
3/16		86.4	36.7	77.2	95.6	74.0
2/16		85.8	33.3	77.4	95.1	72.9
1/16		83.2	33.3	77.6	94.8	72.2
1/32		76.8	26.7	73.4	91.6	67.1

pirically determined mixed-precision scheme is fixed and does not offer a clear method for allocating mixed precision at other compression ratios. In contrast, PRINMIX enables the compression of $\Delta\mathbf{W}$ to arbitrary ratios, offering greater flexibility and broader applicability.

Table 10. The performance of PRINMIX to quantize Qwen2.5-Math-7B-Instruct with different number of calibration data.

Calibration Size	Math500	GSM8K	AVG
16	76.4	94.5	85.5
32	76.2	95.1	85.7
64	76.8	94.3	85.6
128	77.6	94.8	86.2
256	76.0	94.1	85.1

Table 11. The performance of PRINMIX to quantize Qwen2.5-Math-7B-Instruct using calibration data drawn from C4 and Wikitext2.

	Math500	GSM8K	AVG
C4	77.6	94.8	86.2
Wikitext2	76.6	94.8	85.7
MetaMath	75.4	93.6	84.5

C.3. Ablation of Calibration Dataset

Since PRINMIX is a calibration-dependent method, to verify its robustness on calibration, we conducted experiments with different sizes and domains of the calibration dataset to quantize Qwen2.5-Math-7B-Instruct. For calibration on domains, each calibration set contains 128 randomly sampled sequences of length 2048. Due to the insufficient number of sequences of this length in the MetaMathQA dataset, we concatenated multiple question–answer pairs in a few-shot format. To examine the effect of dataset size on calibration, we varied the number of calibration samples on C4 dataset from 16 to 256. The results in Tables 10 and 11 demonstrate that PRINMIX performs well on all calibration setups. The average performance gap is within 2.0%, confirming PRINMIX’s robustness.

C.4. Time For Quantization

Table 12. Time cost (in seconds) for “Simulation”, “Optimization”, and “Quantization” for one transformer block on the Qwen2.5-Math-7B-Instruct model, which consists of 28 blocks.

		Simulation	Optimization	Quantization	Total
PRINMIX	Q_proj	3.1		1.0	134.3
	K_proj	3.1	17.5	1.0	
	V_proj	3.1		1.0	
	O_proj	4.0	11.5	1.5	
	Up_proj	3.3	20.5	2.8	
	Gate_proj	3.3		2.8	
	Down_proj	19.7	24.1	11.0	

In this section, we evaluate the quantization time of PRINMIX within a single transformer block. PRINMIX determines the mixed-precision quantization strategy by minimizing quantization loss, formulated as a 0/1 integer linear programming problem. To clarify the computational overhead, we decompose the quantization time into three components. The first is “simulation time”, which reflects the cost of estimating quantization loss under different bit-widths. The second is “optimization time”, incurred when solving the 0/1 integer linear programming problem. The third is the “quantization time” itself, representing the cost of quantizing each linear layer according to the selected strategy. The corresponding results for one transformer block of Qwen2.5-Math-7B-Instruct, which contains 28 blocks in total, are summarized in Table 12. As shown in Table 12, most of the quantization time is spent on “simulation” and “optimization”. For example, the “simulation” and “optimization” times in Q, K, and V_proj are 9.3s and 17.5s, respectively, while the quantization time only takes 3.0s. Specifically, simulation time increases with the number of columns, while optimization time grows with the number of rows.

Overall, although PRINMIX requires 1.1 hours for 7B models and 2.4 hours for 14B models on a single L20 GPU, this is acceptable.

Accelerating the Optimization Time. As illustrated in Table 12, solving the optimization problem constitutes the primary bottleneck, dominating the total quantization time. To mitigate this overhead, we propose accelerating the ILP solving process through two main avenues: ① increasing the ILP solving speed, and ② constraining the solution space. Specifically, regarding ①, while we employ open-source solvers in this study, switching to a commercial solver like COPT (Ge et al., 2023) can yield a $6\times$ speedup. Furthermore, for ②, the process can be accelerated by limiting the number of candidate bit-widths (e.g., reducing candidates from 8 to 4). Our experiments in Appendix C.5 demonstrate that PRINMIX performs consistently well with different numbers of candidate bit-widths.

These methods significantly enhance PRINMIX’s efficiency in practical deployment. Leveraging the acceleration strategies yields a $4x$ speedup in solving the optimization problem. Consequently, the quantization process for PRINMIX only takes 0.5 hours for 7B models and 1.2 hours for 14B models, representing a 50% reduction in temporal overhead.

C.5. Sensitivity to the Number of Candidate Bit-widths

In this section, we investigate the sensitivity of PRINMIX in the number of candidate bit-widths. We construct the candidates incrementally from $\{0, 2, 3, 4\}$ to $\{0, 2, 3, 4, 5, 6, 7, 8\}$ and quantize Qwen2.5-Math-7B-Instruct at $\alpha = 1/16$ in these 5 different configurations. As shown in Table 13, the performance gap between the best and worst average score is 0.6%, which demonstrate that PRINMIX is robust on the number of candidate bit-widths.

Table 13. Performance of PRINMIX using incrementally expanded candidate bit-widths.

Candidate Bit-widths	Qwen2.5-Math-7B-Instruct		
	Math500	GSM8K	AVG
$\{0, 2, 3, 4\}$	76.7	94.2	85.5
$\{0, 2, 3, 4, 5\}$	77.1	94.0	85.7
$\{0, 2, 3, 4, 5, 6\}$	76.9	94.5	85.5
$\{0, 2, 3, 4, 5, 6, 7\}$	77.3	94.4	85.9
$\{0, 2, 3, 4, 5, 6, 7, 8\}$	77.7	94.6	86.2

C.6. Inference Speed and Memory Cost

To demonstrate the impact of PRINMIX on inference speed and memory cost, we implement a simple Triton (Tillet et al., 2019) kernel for PRINMIX. We compare our kernel with naive aligned models. Since there is no packing function of Delta-CoMe, we use our packing function and kernel for the Delta-CoMe method.

Following the setup in Yao et al. (2024), we assess the end-to-end system performance under varying arrival rates and request distributions. We consider two types of model popularity distribution: 1) Uniform: all models are equally popular. 2) Skewed: model popularity follows a Zipf- α distribution. We evaluate the performance when serving 32 model variants of Qwen2.5-7B. Requests are sent to the serving system at a variable Poisson arrival rate (λ). To simplify, each request consists of 512 tokens, with the model generating one token as its response. We run the simulations for 100 seconds across different arrival rates and model distributions, measuring performance using two metrics: 1) end-to-end latency averaged over all requests; 2) Throughput, number of requests processed per second. All experiments are conducted on a single L40 GPU, with 28G of memory for storing models and the remaining memory for inference.

As shown in the Table 14, PRINMIX improves the throughput $6x$ and decreases end-to-end $100x$ compared to the naive method, because rather than loading the whole full-precision parameters, PRINMIX quantizes the delta-parameters so that a GPU can load more delta-parameters and switch them easily between CPU and GPU.

C.7. Analyzing the Bit Allocation Results

We investigate the bit allocation results across different weight types and layers using the Qwen2.5-Math-7B-Instruct model. Figure 4 shows the memory allocated for each bit-width. Overall, the bit allocation results for different weight types and layers are different. The V_Proj, K_Proj and O_proj in the self-attention layer exhibit a similar allocation trend. For the other four weight types, the bit allocation results differ. For instance, Down_Proj allocates more 2-bit units at the beginning compared to other weight types.

Delta-CoMe (Ping et al., 2024) empirically posits that singular vectors corresponding to larger singular values are more significant and, therefore, necessitate higher-bit representations. We further examine whether PRINMIX adheres to this assumption, specifically by using singular values alone to evaluate importance. We compute the Kendall rank correlation

Principled SVD-based Delta Compression via Quantization Error Minimization

Table 14. The Throughput and End-to-end system performance under varying arrival rates and request distributions when serving 32 model variants of Qwen2.5-7B.

	$\lambda = 0.5$		$\lambda = 1.0$	
	Throughput(req/s)	E2E(s)	Throughput(req/s)	E2E(s)
Zipf ($\alpha = 1.5$)				
Naive	0.21	52.42	0.18	198.48
Delta-CoMe	0.42	0.55	0.87	0.68
PRINMIX	0.42	0.52	0.87	0.62
Uniform				
Naive	0.07	253.93	0.08	481.42
Delta-CoMe	0.42	0.81	0.86	1.44
PRINMIX	0.42	0.79	0.86	1.17

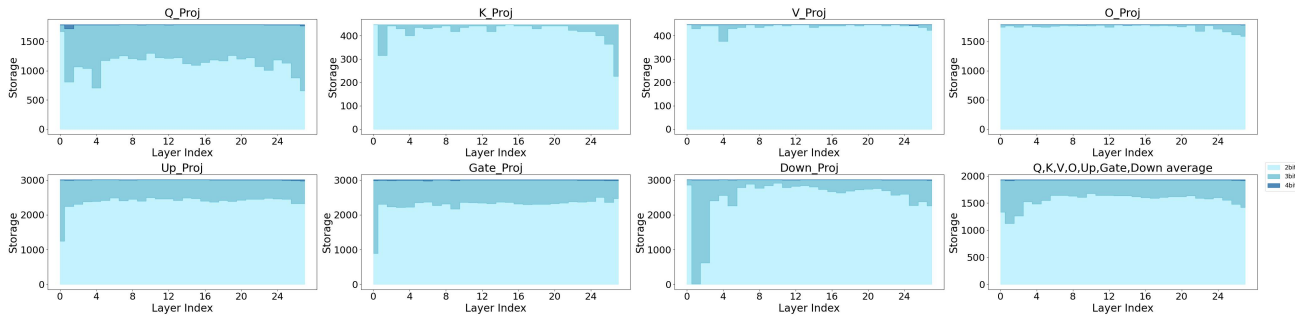


Figure 4. GPU memory usage with quantization bits across layers of Qwen2.5-Math-7B-Instruct.

coefficient τ , between the bit sequence and the singular value sequence for each \mathbf{W} . The coefficient is a measure of rank correlation, ranging from -1 to 1, reflecting the similarity of the orderings of the data when ranked by each of the quantities. If the method strictly adhered to the assumption of using singular values alone for importance assessment, singular vectors with larger singular values would always receive higher bit-width, resulting in a consistent $\tau = 1$ across all \mathbf{W} . However, for the DeepSeek-R1-Distill-Qwen-7B model with PRINMIX, we observe a τ of 0.95 for the \mathbf{W} of the key projection at layer 28. This indicates that PRINMIX goes beyond singular values, taking into account both the “scaling” term and the “difference” term.

C.8. Analyzing the Quantization Error Across Weight Types and Layers

Table 15. Average quantization error ($\times 1e2$) across different type of linears with Eq. (1). “Low”, “Mid”, and “High” denote the first 9 layers, layers 9 to 17, and the last 10 layers, respectively. “All” and “Out” denote the average error across all activations and the average error of the top 1% of activations.

Param		Q_proj						Param		K_proj					
Layer		Low		Mid		High		Layer		Low		Mid		High	
Type	All	Out	All	Out	All	Out	Type	All	Out	All	Out	All	Out		
Low-Rank	0.26	0.32	0.54	0.76	1.33	1.64	Low-Rank	0.06	0.07	0.11	0.13	0.19	0.29		
BitDelta	0.18	0.37	0.27	0.37	0.68	1.00	BitDelta	0.03	0.03	0.05	0.06	0.08	0.12		
Delta-CoMe	0.13	0.14	0.32	0.41	0.81	0.91	Delta-CoMe	0.03	0.03	0.06	0.07	0.12	0.21		
PRINMIX	0.10	0.11	0.25	0.32	0.64	0.73	PRINMIX	0.03	0.03	0.05	0.07	0.10	0.18		
Param		V_proj						Param		O_proj					
Layer		Low		Mid		High		Layer		Low		Mid		High	
Type	All	Out	All	Out	All	Out	Type	All	Out	All	Out	All	Out		
Low-Rank	0.03	0.03	0.06	0.08	0.39	1.11	Low-Rank	0.23	0.40	0.70	1.54	8.52	69.00		
BitDelta	0.01	0.01	0.03	0.03	0.18	0.69	BitDelta	0.10	0.14	0.28	0.46	10.44	895.98		
Delta-CoMe	0.02	0.02	0.04	0.05	0.24	0.85	Delta-CoMe	0.08	0.13	0.32	0.47	3.53	17.02		
PRINMIX	0.02	0.02	0.04	0.05	0.21	0.67	PRINMIX	0.07	0.12	0.30	0.45	3.18	22.31		
Param		Up_proj						Param		Gate_proj					
Layer		Low		Mid		High		Layer		Low		Mid		High	
Type	All	Out	All	Out	All	Out	Type	All	Out	All	Out	All	Out		
Low-Rank	4.78	4.50	2.67	3.18	13.70	14.95	Low-Rank	6.35	3.85	3.16	0.72	13.53	4.02		
BitDelta	4.71	3.85	1.19	1.32	13.30	11.61	BitDelta	9.01	4.47	1.60	0.65	10.32	5.87		
Delta-CoMe	2.10	2.08	1.60	1.90	7.67	9.37	Delta-CoMe	2.64	2.90	1.88	0.84	7.73	3.02		
PRINMIX	1.83	1.74	1.36	1.59	6.58	8.89	PRINMIX	2.28	2.22	1.57	0.59	6.65	2.07		
Param		Down_proj						Param		AVG					
Layer		Low		Mid		High		Layer		Low		Mid		High	
Type	All	Out	All	Out	All	Out	Type	All	Out	All	Out	All	Out		
Low-Rank	1.05	5.52	3.28	4.94	110.20	7470.34	Low-Rank	1.82	3.67	1.50	2.84	21.12	1890.34		
BitDelta	1.21	2.35	0.87	1.45	115.60	11735.05	BitDelta	2.18	2.81	0.61	1.08	21.51	3162.58		
Delta-CoMe	0.33	1.86	1.05	1.57	32.66	1851.91	Delta-CoMe	0.76	1.79	0.75	1.33	7.54	470.82		
PRINMIX	0.31	1.62	1.02	1.43	30.30	1669.95	PRINMIX	0.66	1.46	0.66	1.12	6.81	426.20		